Searching for monocular microsaccades - a red Hering of modern eye trackers?

Marcus Nyström[a,*], Richard Andersson[b,c], Diederick C. Niehorster[a,d], Ignace Hooge[e]

[a] *Lund University Humanities Lab, Lund, Sweden.*
[b] *IT University of Copenhagen, Copenhagen, Denmark.*
[c] *Lund University Cognitive Science, Lund, Sweden.*
[d] *Dept. of Psychology, Lund University, Lund, Sweden.*
[e] *Experimental Psychology, Helmholtz Institute, Utrecht University, Utrecht, the Netherlands.*

Abstract

Despite early reports and the contemporary consensus on microsaccades as purely binocular phenomena, recent work has proposed not only the existence of monocular microsaccades, but also that they serve functional purposes. We take a critical look at the detection of monocular microsaccades from a signal perspective, using raw data and a state-of-the-art, video-based eye tracker. In agreement with previous work, monocular detections were present in all participants using a standard microsaccade detection algorithm. However, a closer look at the raw data invalidates the vast majority of monocular detections. These results again raise the question of the existence of monocular microsaccades, as well as the need for improved methods to study small eye movements recorded with video-based eye trackers.

Keywords: Microsaccades, monocular, eye-tracker data

1. Introduction

Even when trying to keep your eyes as still as possible when fixating an object, the eyes are moving nonetheless. Such fixational eye movements comprise tree types: slow drifts, fast 'jerks' known as microsaccades, and high-frequency tremor (Martinez-Conde et al., 2004). Although the function of fixational eye movements is debated, recent experimental findings propose a range of possible implications for vision (for reviews, *cf.* Collewijn & Kowler, 2008; Rolfs, 2009; Martinez-Conde et al., 2013; Rucci & Victor, 2015).

Historically, microsaccades have, in agreement with larger voluntary saccades, been considered binocular eye movements with amplitudes between a few minutes of arc and up to one degree (Krauskopf et al., 1960; Collewijn & Kowler, 2008; Rolfs, 2009; Martinez-Conde et al., 2009, 2013; Poletti & Rucci, 2016), even though different opinions exist about the 'true' range of amplitudes (Collewijn & Kowler, 2008; Nyström et al., 2014). Microsaccades have distinct shapes consisting of acceleration and deceleration phases terminated by an overshoot (Ditchburn & Foley-Fisher, 1967). Figure 1 shows the horizontal (top) and vertical (bottom) components of eye-tracker signals recorded from the left (L) and right (R) eyes of a person fixating a small dot. Four microsaccades are marked in green, and the third microsaccade from the left hand side is also illustrated in the spatial domain (Figure 2). As can be seen from the figures, microsaccades are small, and rarely go in straight lines between their onsets and offsets, and are characterized by significant curvature. Even though the exact properties of data recorded from a microsaccade is system-dependent, this description of microsaccade dynamics seems to be universal across the most common recording techniques (Nyström et al., 2014; McCamy et al., 2015).

It is generally agreed that microsaccades are binocular, and the standard approach in the field is to reject microsaccades that are detected in only one eye (Engbert & Mergenthaler, 2006; Troncoso et al., 2008). Still, all major reviews on microsaccades over the past years include a few studies that report the existence of monocular microsaccades, i.e., microsaccades that occur only in one eye without being accompanied with a simultaneous microsaccade in the other eye. However, such monocular microsaccades are typically discarded as noise resulting from the instrument. Collewijn & Kowler (2008), for instance, write that

> A telltale sign of the problematic detection of microsaccades in video-tracker signals was the occurrence of monocular saccades in the recordings

and further cite Martinez-Conde et al. (2006) who report that binocular microsaccades were more effective in counteracting Troxler fading compared to monocular ones "reinforcing the suspicion that the monocular saccades might be noise." Importantly, Martinez-Conde et al.'s definition of monocular microsaccades was sample-based, meaning that "each millisecond that a microsaccade was in flight was classified as binocular (if both eyes were engaged in a

*Corresponding author
Email addresses: marcus.nystrom@humlab.lu.se (Marcus Nyström), richard.andersson@humlab.lu.se (Richard Andersson), diederick.c.niehorster@humlab.lu.se (Diederick C. Niehorster), i.hooge@uu.nl (Ignace Hooge)

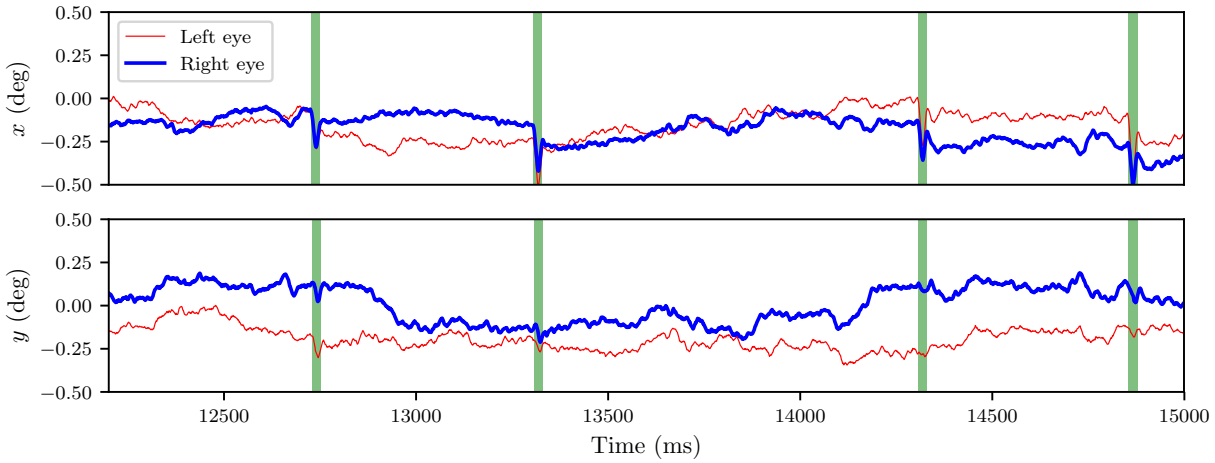

Figure 1: Example of horizontal (top) and vertical (bottom) components of binocular eye-tracker data. Microsaccade intervals detected with the algorithm by Engbert & Kliegl (2003b) are marked with green vertical bars. Data were recorded with a video-based eye tracker (EyeLink 1000 Plus) at 1000 Hz from a participant fixating a 0.33 degree dot on a computer screen.

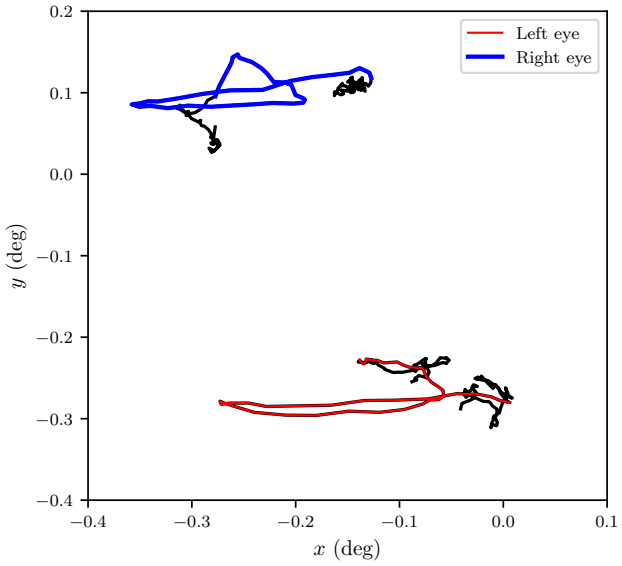

Figure 2: xy-plot of the third microsaccade from Figure 1. The microsaccade is mainly horizontal and displaces the eye in the leftward direction. Notice the large overshoot in relation to the displacement of the microsaccade.

microsaccade) ... or monocular (if only one eye was engaged in a microsaccade)". As such, monocular microsaccades could represent samples where the movement in one eye starts earlier or later than in the other eye.

Given the relatively higher precision of the invasive, analogue eye tracker of the past, it is perhaps unsurprising that monocular microsaccades recorded with modern video eye trackers are received with some skepticism. Using the optical lever technique, Krauskopf et al. (1960) report median microsaccade amplitudes in the range of 2-4 min arc., and write

> The most striking characteristic of our eye movement records is the synchrony of saccades in the two eyes. Examination of records obtained during 80 min of binocular fixation failed to reveal one unequivocal case of a saccade in one eye unaccompanied by a saccade in the other.

This is in line with more recent investigations of binocular coordination during fixation from Møller et al. (2002) who write that

> All microsaccades for all test persons were performed simultaneously and individually with an almost identical amplitude in the right and left eye

Importantly, however, Møller et al. (2002) report average microsaccade amplitudes between 0.3–1.1 degrees in their EyeLink I data, and argue that the larger values may be because a chin-, and forehead rest is used instead of a bitebar, as used in earlier studies.

Using the same eye tracker model—the EyeLink I—but in strict contrast with these findings, Engbert & Kliegl (2003a) found almost half (42%) of the microsaccades to be monocular. The monocular microsaccades had smaller amplitudes than binocular microsaccades, but followed the

same systematic relationship between amplitude and peak velocity—the main sequence—as the binocular ones which, according to Engbert & Kliegl (2003a), makes it unlikely that they merely represent noise. Interestingly, they also found large differences in direction between monocular and binocular microsaccades; while binocular microsaccade were mainly horizontal, the monocular microsaccades had a proportionally larger vertical prevalence.

To test possible mechanisms behind the generation of monocular microsaccades, Kloke et al. (2009) compared data recorded under monocular and binocular viewing. They largely replicated the finding by Engbert & Kliegl (2003a) and reported 34% monocular detections. However, they did not find any statistical differences in microsaccade properties due to the different viewing conditions. Regarding the existence of monocular microsaccades they argue that "it still seems more probable that this is a weakness of the detection procedure than a real physiological phenomenon" attributing many of the monocular detections to naturally varying velocity between the two eyes.

Using the EyeLink 1000, which in contrast to the head-mounted EyeLink I and II is desktop-mounted, Gautier et al. (2016) recently provided some compelling evidence that monocular microsaccades exist and also have functional implications. In agreement with earlier studies, they report of a proportion of monocular microsaccades between 9 and 41%, depending on the parameter settings of the microsaccade detection algorithm. Importantly, they found that the proportion of monocular microsaccades changed as a function of contrast during a visual detection task such that a proportional increase occurred at the visual threshold. Gautier et al. (2016) argue that monocular microsaccades may have a functional role to facilitate binocular summation by decreasing vergence errors.

Even though recent work has challenged the contemporary consensus that microsaccades are binocular and argued vigorously for the existence and function of monocular microsaccades, no satisfying explanation for the large discrepancies in results over the past decades has been provided. In the current paper, we approach the problem from a signal perspective and ask whether monocular detections in the gaze signal remain credible even after closer scrutiny of the raw data they originate from. 'Monocular detections' refer in this paper to microsaccade candidates detected in one eye, but without a temporally overlapping microsaccade candidate detected in the other eye. The main contribution of this paper is that, unlike traditional studies using video-based eye trackers, not only the gaze signal is considered, but also the raw pupil and corneal reflection (CR) signals are inspected. These are the signals from which the gaze signal is constructed (Merchant et al., 1974; Young & Sheena, 1975). The advantage of using these signals is that they are accessed before any calibration or filtering of the gaze-, and velocity signals are applied, which is critical when attempting to detect tiny eye movements barely exceeding the system noise (see e.g., Nyström et al., 2015, 2016; Hooge et al., 2016). In addition,

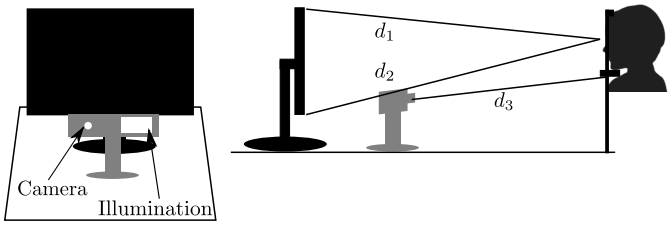

Figure 3: Geometric setup. Left: front view of setup from the position of the participant's eyes. Right: side view of distances from the eyes to the top if the screen (d_1 = 81 cm), the bottom of the screen (d_2 = 83 cm), and the camera (d_3 = 52 cm).

binocular data recorded at 1000 Hz from the most recent addition of the EyeLink-family, an EyeLink 1000 Plus, is used, which adds a twofold increase in temporal resolution compared to its predecessor used in the majority of other recent microsaccade studies. Due to this increase, smaller microsaccades can be described in greater detail.

In this paper, we explore the degree to which monocular microsaccades detected through conventional analysis is supported after more in-depth analyzes of more raw estimates of eye movements. The paper starts with a replication, where we in agreement with previous work find monocular detections in all participants and eyes. After a more critical, in-depth analysis of the gaze data, raw pupil-, and CR data were presented where monocular detections from the algorithm are accepted or rejected after visual inspection. Very few algorithmically detected monocular microsaccades survived closer scrutiny. Finally, manual coding of a subset of the raw data was performed to ensure that no potential monocular microsaccades had been missed by the detection algorithm. The reasons and implications of these finding are probed in the discussion.

2. Methods

2.1. Participants

Eight participants (two female) were recorded (range 26–41 years, P_1 and P_2 were authors). They had normal or corrected-to-normal vision, and no known problems with their binocular vision. The experiment was conducted in agreement with the Code of Ethics of the World Medical Association (Declaration of Helsinki), and informed consent was taken from all participants.

2.2. Stimulus and Apparatus

Binocular eye movements were recorded at 1000 Hz using the EyeLink 1000 Plus (host software v. 5.09) set up according to Figure 3.

The center of mass tracking mode was used and both heuristic filters were switched off. Besides calibrated gaze coordinates, centers of the pupil-, and CR given in the eye camera's coordinate system were recorded by the eye tracker.

The stimulus consisted of a small white cross (0.33 deg) presented on a mid-gray background (pixel grayscale value

128) and was presented on an ASUS VG248QE monitor with a resolution of 1920×1080 pixels (53×30 cm) and a refresh rate of 144 Hz. PsychoPy (Peirce, 2007, 2008, v. 1.83.01) was used for stimulus presentation and the EyeLink Dev Kit (v. 1.11.571) was used to communicate with the EyeLink Host computer.

2.3. Procedure

Participants were seated and asked to place their heads in a chin- and forehead rest and sit as still as possible and minimize the amount of blinking during the experiment. Using the 35 mm lens and positioning the desktop mount as recommended by the manual, it was not possible to adjust the camera zoom such that the CR was minimized in both eyes, which is the recommended way to achieve a sharp eye image. A likely reason is the camera and illumination are off center relative to the eyes. We solved this problem by adjusting the zoom level such that the CRs in both eyes got approximately the same size. At the same time, we moved the camera to get as similar pupil, and CR threshold values as possible between the eyes. Participants were calibrated with the standard 9-point calibration, followed by a 9-point validation. The accuracy across all participants, eyes, and calibration targets was 0.33 degrees ($SD = 0.18$) and spanned the interval $[0.03, 0.97]$ degrees. Twentyfour (16%) accuracy values were above 0.5 degrees.

A recording consisted of two blocks, each where participants fixated the white cross continuously for 200 s (participants P_1–P_4) or 100 s (participants P_5–P_8). A short break followed by a re-calibration was done prior to the onset of the second block. The illuminance was constant and came from overhead fluorescent lighting. When a photometer sensor (Hagner ScreenMaster) was positioned at the location corresponding to participants' eyes during the experiment and directed toward the screen, a reading of 197 lux was reported. The screen luminance measured with the same photometer was 80 cd/m^2.

2.4. Data Analysis

Similar to earlier studies, microsaccades were detected using the algorithm by Engbert & Kliegl (2003b) with the parameters $\lambda = 6$ and a minimum microsaccade duration of 8 ms. If the separation between two microsaccades was less than 20 ms, they were merged into one with a duration spanning from the onset of the first microsaccade to the offset of the second one (Martinez-Conde et al., 2006).

The filter used to compute velocity proposed by Engbert & Kliegl (2003b) and Engbert & Mergenthaler (2006) is defined as

$$v_n = \frac{x_{n+2} + x_{n+1} - x_{n-1} - x_{n-2}}{6\Delta t}. \quad (1)$$

While their algorithm was developed for 250 and 500 Hz data, we use the following version of the filter at 1000 Hz (Bahill et al., 1982).

$$v_n = \frac{x_{n+3} - x_{n-3}}{6\Delta t}. \quad (2)$$

Unlike the majority of previous work on microsaccades using the EyeLink family of eye trackers, we turned the two heuristic filters off to record 'raw' gaze data. Leaving the raw gaze data unfiltered with the above parameters clearly did not work, and typically produced rates below 0.1 microsaccade/s. Therefore, we apply a third order Savitzky Golay filter of length 21 samples (21 ms) prior to microsaccade detection (Savitzky & Golay, 1964; Nyström et al., 2013). This filter length was selected since it maximized the rate of detected binocular microsaccades; smaller and larger values produced lower rates (*cf.* the Appendix for an example).

Although the majority of the previous results is based on the algorithms by Engbert & Kliegl (2003b) and Engbert & Mergenthaler (2006), we also include a more recent algorithm for comparison designed "not to discard potential monocular microsaccades" (Otero-Millan et al., 2014)[1]. Since no microsaccade was detected for one of the participants using the Otero-Millan et al. (2014)-algorithm with default settings, we changed the value on line 103 in `SaccadeDetectorCluster` from 0.2 to 0.1. This modification gave reasonable results for this participant without changing the results of the other participants. The reason the default value did not work is likely the small microsaccades produced by this participant (P_1) [2].

Microsaccades were detected in each eye separately using the filtered gaze data. Those with a temporal overlap of at least one sample (1 ms) were considered binocular. Properties of the binocular detections (amplitude, peak velocity, direction) are represented by averages of monocular properties in the left and right eyes.

In the following, results refer to detections from the Engbert & Kliegl (2003b) algorithm, unless explicitly stated otherwise. The algorithms are abbreviated as the EK (Engbert & Kliegl, 2003b) and the OM (Otero-Millan et al., 2014) algorithms, respectively.

3. Results

3.1. Microsaccade detection using the gaze signals

Tables 1 and 2 show a summary of signal properties and microsaccades statistics for each participant. As can be seen from the first table, the precision of the eye-tracker data is rather consistent across the participants, even though variation exists both across participants and eyes. Note the difference between raw and filtered data of about one order of magnitude. As expected, the root mean square (RMS) of intersample distances is more influenced by filtering compared to the standard deviation (SD).

In contrast, the individual variation in rate, amplitude, and the proportion of monocular detections is large (Table 2). In total, 3559 microsaccades were detected by the

[1] Source code available from `http://smc.neuralcorrelate.com/sw/microsaccade-detection/` (retrieved 2017-03-22).

[2] Personal communication with Jorge Otero-Millan.

Table 1: Properties of the eye-tracker signals for each participant (PID) and eye (L/R). Results are given as the root mean square (RMS) of inter-sample distances and the standard deviation (SD) of gaze data, and are presented separately in the horizontal (x) and vertical (y) direction. Values are computed as follows: first the mean values of RMS and SD are computed within 200 ms, non-overlapping windows. The median of all means are presented below. All numbers are in degrees.

PID	Eye	Filtered	RMSx	RMSy	SDx	SDy
P_1	L	N	0.041	0.044	0.041	0.042
		Y	0.004	0.004	0.030	0.028
	R	N	0.036	0.043	0.035	0.046
		Y	0.003	0.004	0.025	0.034
P_2	L	N	0.058	0.048	0.055	0.047
		Y	0.006	0.005	0.039	0.033
	R	N	0.050	0.055	0.045	0.051
		Y	0.005	0.005	0.030	0.033
P_3	L	N	0.057	0.059	0.052	0.049
		Y	0.005	0.005	0.032	0.028
	R	N	0.049	0.061	0.049	0.059
		Y	0.005	0.006	0.023	0.038
P_4	L	N	0.040	0.041	0.051	0.056
		Y	0.004	0.005	0.043	0.048
	R	N	0.050	0.052	0.044	0.052
		Y	0.005	0.005	0.027	0.039
P_5	L	N	0.045	0.044	0.042	0.040
		Y	0.004	0.004	0.028	0.027
	R	N	0.045	0.049	0.038	0.046
		Y	0.004	0.005	0.023	0.032
P_6	L	N	0.041	0.044	0.045	0.046
		Y	0.004	0.004	0.036	0.035
	R	N	0.042	0.050	0.041	0.051
		Y	0.004	0.005	0.028	0.037
P_7	L	N	0.059	0.068	0.055	0.067
		Y	0.006	0.007	0.034	0.046
	R	N	0.060	0.071	0.052	0.078
		Y	0.005	0.007	0.032	0.060
P_8	L	N	0.029	0.032	0.034	0.044
		Y	0.003	0.003	0.027	0.039
	R	N	0.026	0.030	0.035	0.041
		Y	0.003	0.003	0.030	0.036

Table 2: Properties of detected microsaccades for each participant (PID) using the algorithm by Engbert & Kliegl (2003b). The number (N), rate (1/s), and amplitude (M±SD) in minutes are presented for monocular detections (left [L] and right [R] eyes) and binocular detections (B). Note that participants P_1 through P_4 were recorded twice as long as the last four participants, explaining the overall lower number of detected microsaccades for P_5 through P_8.

PID	Eye	N	Rate	Amp (M ± SD)
P_1	L	34	0.08	7.63 ± 2.17
	R	71	0.18	8.30 ± 4.25
	B	557	1.37	8.76 ± 3.64
P_2	L	55	0.14	8.25 ± 4.04
	R	34	0.08	10.14 ± 3.21
	B	773	1.90	27.02 ± 18.43
P_3	L	11	0.03	7.33 ± 1.06
	R	8	0.02	7.51 ± 0.94
	B	208	0.52	17.48 ± 9.98
P_4	L	221	0.54	8.28 ± 2.63
	R	47	0.12	9.29 ± 3.00
	B	424	1.04	11.78 ± 5.71
P_5	L	8	0.04	7.78 ± 1.28
	R	4	0.02	6.77 ± 5.04
	B	152	0.78	19.89 ± 23.71
P_6	L	41	0.21	7.30 ± 2.10
	R	30	0.15	8.32 ± 2.60
	B	342	1.71	13.07 ± 4.75
P_7	L	20	0.11	11.11 ± 3.33
	R	47	0.25	13.05 ± 3.97
	B	167	0.88	14.65 ± 6.26
P_8	L	41	0.21	6.10 ± 1.71
	R	50	0.26	6.56 ± 3.15
	B	217	1.12	14.98 ± 9.88

EK algorithm. Out of these, 2838 (80%) were binocular detections and 721 (20%) monocular detections. This can be compared to the results in Table 3, where microsaccades from the same input signals were detected with the OM algorithm. According to this algorithm there were 3452 microsaccades of which 2565 (74%) were binocular and 887 (26%) were monocular. The vast majority of binocular detections found by one algorithm was also found in the other algorithm; 97% of the detections in the OM algorithm was found in the EK algorithm, while 85% of the detections in the EK algorithm was found in the OM algorithm. In contrast, the corresponding numbers for monocular detections were 34% and 28%. A similar pattern was found when using the F_1-score—the harmonic mean of precision and recall—to compare the algorithms (Hooge et al., in press); the F_1-score for binocular detections was high (0.91) whereas the F_1-score for monocular detections was on average low, 0.31 (left eye: 0.34, right eye: 0.27), indicating a poor agreement between the algorithms. Like the EK algorithm, the OM-algorithm clearly was not suitable to process unfiltered gaze data (cf. Table A.6); the binocular detection rate was reduced by half whereas the monocular detection rates experienced a five-fold increase compared to the results based on filtered data (Table 3).

Microsaccade directions are illustrated in Figure 4. In line with previous research, the majority of binocular microsaccades (green) were performed in the horizontal direction, whereas monocular detections were less restricted to the horizontal direction.

Typically, a systematic relationship between amplitude and peak velocity—known as the *main sequence* (Bahill et al., 1975)—has been interpreted as evidence that microsaccade detection has been successful. In Figure 5(a), the main sequence for monocular and binocular microsaccades is shown, and a linear relationship can be discerned. However, there is a larger variation around the linear trend compared to many of the results previously reported. The data points off the main sequence represent microsaccades with high peak velocities relative to their amplitudes. Such examples likely represent a 'double saccadic pulse', which Abadi & Gowen (2004) describe as a saccadic intrusion that "consists of an initial saccade away from fixation fol-

Table 3: Properties of detected microsaccades for each participant (PID) using the algorithm by Otero-Millan et al. (2014). The number (N), rate (1/s), and amplitude (M±SD) in minutes are presented for monocular detections (left [L] and right [R] eyes) and binocular detections (B). Note that participants P_1 through P_4 were recorded twice as long as the last four participants, explaining the overall lower number of detected microsaccades for P_5 through P_8.

PID	Eye	N	Rate	Amp (M ± SD)
P_1	L	58	0.14	8.10 ± 3.66
	R	71	0.18	8.62 ± 3.87
	B	554	1.37	9.86 ± 3.74
P_2	L	56	0.14	17.11 ± 8.29
	R	55	0.14	19.18 ± 5.84
	B	612	1.50	42.39 ± 24.74
P_3	L	13	0.01	11.22 ± 6.65
	R	7	0.02	15.08 ± 7.02
	B	196	0.49	20.25 ± 9.16
P_4	L	151	0.37	10.26 ± 4.27
	R	85	0.21	9.72 ± 4.55
	B	404	10.99	13.66 ± 6.39
P_5	L	4	0.02	9.84 ± 2.48
	R	7	0.04	9.42 ± 3.03
	B	137	0.70	24.75 ± 24.04
P_6	L	25	0.13	10.50 ± 3.76
	R	39	0.20	10.39 ± 3.19
	B	310	1.55	14.56 ± 5.60
P_7	L	210	1.11	7.25 ± 3.31
	R	71	0.37	14.18 ± 4.90
	B	171	0.90	15.60 ± 11.24
P_8	L	12	0.06	11.72 ± 4.22
	R	34	0.18	10.34 ± 3.88
	B	189	0.98	18.26 ± 10.65

lowed immediately by a return saccade back to fixation". Clearly such microsaccades with high velocity and very low displacement would not lay on the main sequence. For comparison, the same data are presented in Figure 5(b) where the amplitudes were computed as the maximum distance between any two samples during the detected microsaccade. Using this metric, the vast majority of data points lay on the main sequence.

The peak velocity of the left eye (red) compared to the right eye (blue) is plotted in Figure 6, for both binocular (green) and monocular detections. In agreement with Gautier et al. (2016), it can be verified that monocular detections occur where velocities are low and differ between the eyes.

The above results are mainly replications of previous work using similar instrumentation; monocular detections were found in data from all participants and eyes, but less frequently than binocular ones. They were smaller in amplitude compared binocular detections and had a larger vertical prevalence (Engbert & Kliegl, 2003a; Kloke et al., 2009; Gautier et al., 2016). So can we now safely conclude that monocular microsaccades exist based on the recorded data?

One hypothesis is that monocular detections are the results of imperfection in the detection procedure, and that

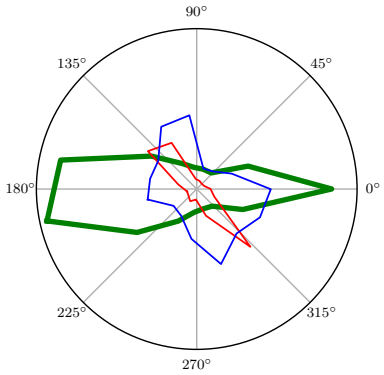

Figure 4: Direction of microsaccades detected in both eyes (thick green line), only in the left eye (red), and only in the right eye (blue). The radii have been scaled for display purpose. Zero (0) degrees indicate microsaccades in the rightward direction.

monocular detections are in fact binocular saccades where the detection in one eye has failed. In this case, there should be a slower, but similarly directed, movement in the eye where a microsaccade was not detected. Figure 7 shows the difference in direction (φ) between the eyes, where monocular (top) and binocular (bottom) detections are presented separately. Clearly, the angular difference is small in many of the monocular and binocular detections; for the latter, only a small percentage (11%) differs by more than 45 degrees. Similar numbers for monocular detections are 54% (left eye) and 37% (right eye). It should be noted that one of the participants (P_4) is responsible for the majority of large angular differences ($|\varphi| > 90$ degrees) in the left eye, explaining the bimodal appearance of the histogram in Figure 7. Importantly, binocular microsaccades become more equally directed as the amplitude increases, as illustrated in Figure 8. Extracting a subset of binocular detections of a similar amplitude range as the monocular detections (< 15 min arc) increases the percentage of binocular detections that differs by more than 45 degrees from 11% to 18%. Consequently, given the small amplitudes of monocular detections, a large difference in direction may not be sufficient to disqualify them as binocular events.

3.2. Further insights from raw pupil-, and CR data

It has become increasingly clear over the course of this project that gaze data in combination with standard detection methods can tell us only part of the reason why monocular detections occur. To more closely probe the origin of monocular detections, we revert to 'raw' data, i.e., the unfiltered pupil, and CR signals, which comprise the raw material for the gaze data normally used to detect microsaccades. The advantage of inspecting raw data is twofold: First, potential signal artifacts can be traced to either the CR signal or the pupil signal. Second, potential signal distortion introduced by filtering is a smaller issue in the raw data. In contrast, a detection algorithm generally bases its decisions on a signal that has been filtered twice: first with the internal, heuristic EyeLink filters or other

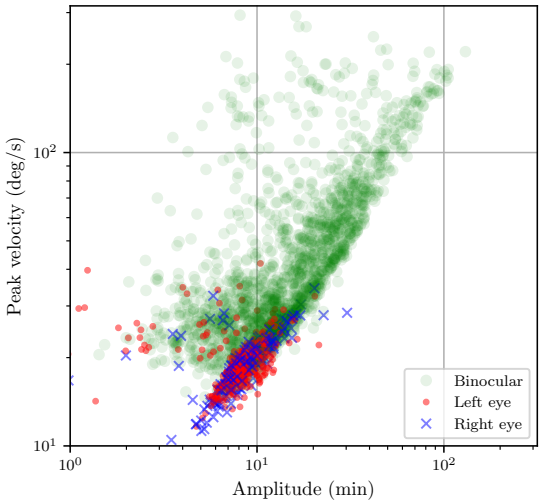

(a) Main sequence plot with amplitude calculated as displacements from the onset to the offset of the detected microsaccade.

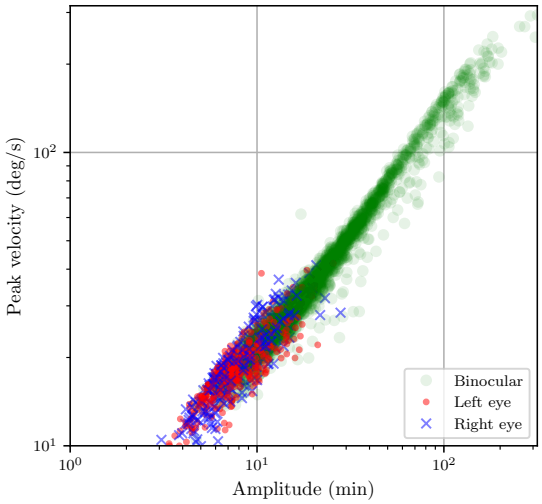

(b) Main sequence plot where the amplitude represents the maximum excursion during the microsaccade, i.e., the displacement plus the overshoot.

Figure 5: Main sequence plots for monocular (red dot - left eye, blue cross - right eye) and binocular (green circles) detections. Each marker represents one detected microsaccade.

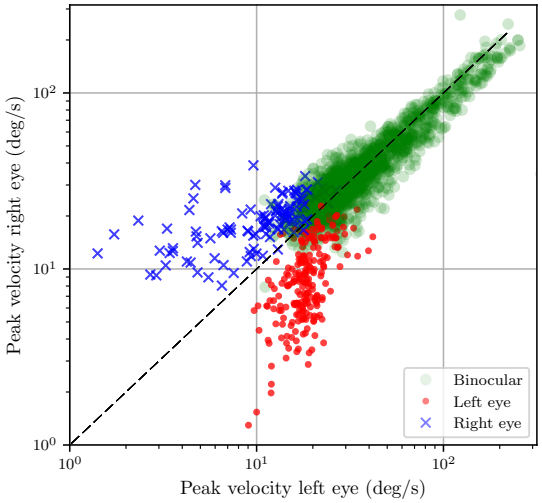

Figure 6: Peak velocity in the left eye (x-axis) versus the right eye (y-axis) for binocular (green circles) and monocular (red dot - left eye, blue cross - right eye) detections. When the detection is monocular, it is compared to the peak velocity from the signal in the other eye during the same time interval.

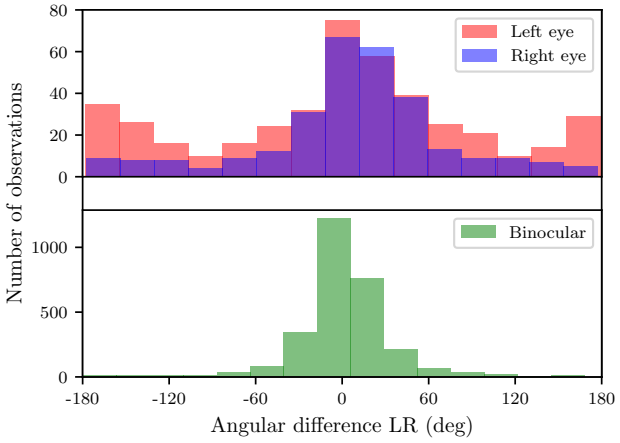

Figure 7: Directional difference between the eyes for monocular (top) and binocular (bottom) detections. An angular difference of zero (0) means that data from the eyes are unidirectional, whereas ±180 means that they go in opposite directions. Even for monocular detections, the eyes are many times rotated in a similar direction.

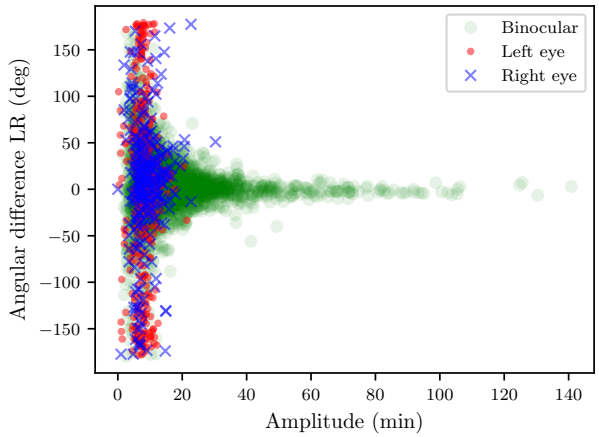

Figure 8: Directional differences between the left and right eyes for monocular detections in the left eye, the right eye, and for binocular detections. Smaller microsaccades are less unidirectional.

filters applied offline to the gaze data, and then with the filter internal to the detection algorithm (Engbert & Kliegl, 2003b; Engbert & Mergenthaler, 2006). It cannot be ruled out that monocular microsaccades are 'fabricated' due to this signal processing.

Figure 9 illustrates the horizontal and vertical components of a monocular detection in the velocity domain (two top panels, marked with purple color), and the corresponding raw data (two bottom panels). Given only the velocity signal, i.e., the information provided to the detection algorithm, it indeed looks like the there is a vertical moment in only one of the eyes. However the raw data (bottom) do not provide any convincing evidence that there is a real difference between the pupil and CR signals in either of the eyes. For comparison; each of the larger, binocular detections, marked with green background, is clearly seen in both the gaze velocity signal and in the raw data.

3.3. Manual inspection

Data from the first four participants were selected for manual inspection. To inspect the candidates most likely to be truly monocular in nature, the monocular detections that differed the most in velocity ($n = 5$) and direction ($n = 5$) between the eyes were extracted for each selected participant and eye. Since some of the monocular detections had large differences in both velocity and direction, 122 of the 160 (4 participants × 2 eyes × 2 blocks × 10 detections) monocular detections made the final selection. Each of these was manually inspected, and classified into one of three categories based on the raw pupil-, and CR-data: 1) binocular 2) monocular, and 3) noise. The first category includes cases where a microsaccade is present in the non-detected eye, but the algorithm has failed to detect it. The second category contains examples where it cannot be ruled out that the microsaccade is genuinely monocular. Finally, the third category represents the case where the monocular detection was the result of noise.

Table 4: Result of manual inspection of a subset of monocular detections using raw pupil and CR signals. The values represent the number of monocular detections considered to be (1) missed binocular microsaccades, (2) monocular microsaccades, (3) or detections due to noise.

Coder ID	No. detections		
	1. Bino.	2. Mono.	3. Noise
C_1	43	4	75
C_2	39	2	81

Table 5: Result of manual inspection of all data from the first block using raw pupil and CR signals. X(Y) represent the number of binocular (X) and monocular (Y) events detected by the human coders C_1 and C_2. For comparison, corresponding results are given for the EK algorithm applied to the gaze velocity signal. PID denotes the participant ID.

PID	Detection method		
	C_1	C_3	EK
P_1	290(2)	295(0)	275(40)
P_2	473(1)	438(0)	400(40)
P_3	113(0)	115(0)	113(6)
P_4	260(0)	264(1)	215(146)

After manual inspection, 3% of the monocular detections were categorized as monocular microsaccades (category 2), 64% as noise and 82 33% as failed detection of binocular saccades (category 1). Individual results from two manual coders are given in Table 4. As can be seen from the table there was a very high agreement across the two coders, and only three of the monocular detections could not be rejected based on inspection of the raw pupil-, and CR data.

To exclude the possibility the monocular microsaccades were present in the data, but missed by the algorithm, further manual coding was performed on raw data to identify potential binocular-, and monocular microsaccades; two coders (C_1, C_3) manually inspected pupil-, and CR data from the first block from all participants. Each block took about 20 min to inspect. Even though the coders were generous in favor of detecting monocular events, only four cases were reported (*cf.* Table 5). These are visualized in the Appendix (Figure A.11). We leave it to the reader to decide whether any of them is a genuine monocular microsaccade. The EK algorithm reported 232 monocular detections for the same data set. All raw data along with the manual annotations[3] used in this paper are publicly available (Nyström, 2017).

4. Discussion

Do monocular microsaccades exist—in disagrement with the contemporary consensus but in line with a few recent studies—or are they artifacts of modern, video-based eye

[3]Three of the authors conducted the manual coding.

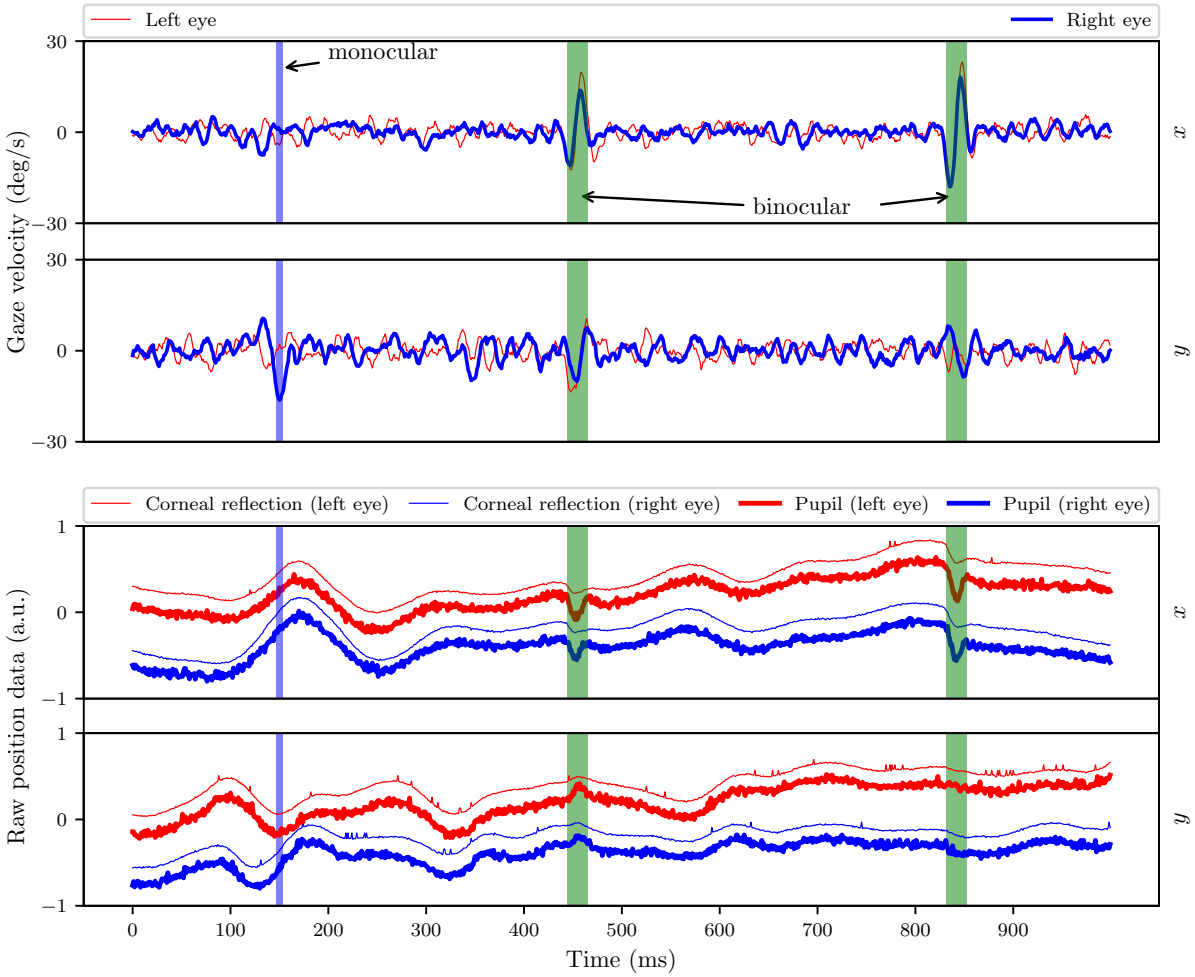

Figure 9: Two top panels: Horizontal (top) and vertical (bottom) gaze velocity signals. Two bottom panels: Horizontal (top) and vertical (bottom) pupil-, and CR position signals. Three algorithmically detected microsaccade candidates are marked with vertical bars. The first (blue) is a monocular detection and the other two binocular detections (green). Notice the slow variation in the pupil-, and CR-signals reflecting a combination of eye drift and (small) head movement relative to the eye tracker.

trackers along with subsequent signal processing? We approached the question from a signal perspective by comparing the results obtained through traditional analysis with manual analyzes and inspection of 'raw' pupil-, and CR data. Previous results were largely replicated, where monocular detections in gaze data were present in all participants and eyes; about one fourth of the detections in our data were monocular. While two common algorithms for microsaccade detection largely agreed on where the binocular microsaccades were located, their monocular detections had a poor overlap. More in-depth analyzes revealed that the majority of monocular detections were either due to noise or missed binocular microsaccades. Only a few cases of the monocular detections could not be immediately rejected after consulting the raw data. Consequently, our results are in line with early reports presenting microsaccades as binocular phenomena, e.g., Krauskopf et al. (1960), but challenge recent findings where monocular detections recorded with similar instrumentation as in this paper not only have been reported as real phenomena, but also have been given visual significance (Gautier et al., 2016).

So why do monocular detections occur? A subset of the monocular detections most 'monocular' in nature, i.e., those with the largest difference in velocity and direction across the eyes, were extracted for manual inspection. About one third of these were missed binocular microsaccades, where only the velocity in one eye reached the detection threshold. Given that the monocular detections were small and close to the detection threshold, it should come as no surprise that there are instances where this situation occurs, for at least two reasons. First, both larger, voluntary saccades and fixational saccades exhibit a natural movement asymmetry between the two eyes, leading to different peak velocities between the right and the left eyes (Collewijn et al., 1988). Second, the signal quality between the two eyes can differ due to, e.g., how difficult they are to track, or different choices/settings made during the instrument setup leading to differences in signal velocities between the eyes. Similar explanations related to both the participant and the instrument apply also to monocular detections originating from noise (2/3 of the cases). Furthermore, it is clear from inspection of the raw data that a few monocular detections can be traced to artifacts in the signal that may be related to imperfections in detecting the centers of the pupil and CR. Since the tracking algorithms are proprietary, it is difficult to know the cause behind these artifacts. However, previous work has seen that "the corneal reflection coming in and out of the pupil can introduce a quick change in the position of the center of mass of the pupil" (Otero-Millan et al., 2014). Since the corneal reflection for reasons of geometry is at slightly different positions in the two eyes (*cf.* Figure 3), and therefore enters and exits the eye at a different moment during the eye movement, it cannot be excluded that the artifact described by Otero-Millan et al. (2014) may in itself cause erroneous monocular detections.

Being able to access the raw pupil-, and CR data provides an excellent way to critically evaluate in more detail why the monocular detections occur, something that would be difficult given only the gaze position-, and velocity-signals, which is the only information available to the detection algorithm. As illustrated in Figure 9, it was not always trivial to map the appearance of a monocular detection in the velocity domain to the corresponding raw pupil-, and CR-signals. There are at least three levels of processing going from the raw signals to the velocity signal that could be responsible for such difficulties: the proprietary calibration function mapping raw pupil-, and CR data to gaze signals, any filter applied to the raw, calibrated gaze data, and the differentiation filter part of the microsaccade detection algorithm.

In this paper, we have chosen a certain set of parameters used for filtering of data and detection of microsaccades. In agreement with Gautier et al. (2016), we found that different values of these parameters can lead to substantial changes in microsaccade statistics, including the rate of monocular microsaccades. Most parameters in this paper were set in agreement with previous work. The exception was the length of the Savitzy-Golay filter, which was set to 21 samples. This length maximized the number of detected binocular microsaccades, led to a high agreement with the OM-algorithm using another type of filter to compute velocities, and provided reasonable results when data were manually inspected. Much smaller or larger window lengths provided binocular results that were simple not credible (see Appendix). Importantly, monocular detections were *always* found for all tested parameters settings within a reasonable range. Irrespective of their exact numbers or positions, however, nearly all of them would always be rejected due to their absence in the raw pupil-, and CR-signal.

It should be noted that the large number of erroneous monocular detections seems to be a problem related to signal processing rather than a problem of the video eye tracker per se. Using raw pupil-, and CR data in combination with visual inspection, the signal quality seems high enough to correctly reject monocular detections found with an algorithm operating on the gaze velocity signal. Consequently, there may be room for improvements in future microsaccade detection algorithms by using the raw data directly instead of more processed gaze-, and velocity signals.

Even though our data provide convincing evidence that monocular detections are artifacts of, amongst others, the signal processing and detection algorithms used during analysis, we cannot exclude the possibility that monocular microsaccades occur under different circumstances. An important difference between our work and the work by Gautier et al. (2016) is that they used a bitebar to stabilize participants' heads, whereas the manufacturer provided head-, and chin-rest was used in the current study. It is known from previous work that bitebars can influence both the signal quality and the oculomotor behavior (Skavenski et al., 1979). Also higher level processes are known to influence microsaccades (Siegenthaler et al., 2014), and it cannot be excluded that there are tasks that modulate

monocular eye control.

Gautier et al. (2016) also report that the rate of monocular microsaccades changes with the contrast of a visual stimulus such that a higher proportion of monocular microsaccades is observed around the discrimination threshold. They argue that monocular microsaccades therefore may play a functional role when making fine visual discrimination. The findings of this paper call for alternative interpretations of their data. Even though we could only speculate here, it is known that other properties of microsaccades change in response to varying stimulus contrast, e.g., the rate and amplitude (Rolfs et al., 2008; Scholes et al., 2015), which may well interact with the rate of monocular detections.

Finally, there is recent neurological evidence that points toward separate programming of microsaccades (Cullen & Van Horn, 2011; Van Horn & Cullen, 2012), in disagreement with Hering's law of equal innervation, according to which both eyes are controlled by a common underlying mechanism (King, 2011). Irrespective of whether monocular microsaccades exist, our results show that their prevalence is grossly overestimated in studies using current state-of-the-art video based eye trackers in combination with standard analyzes of the data.

4.1. Conclusions

About a quarter of all microsaccades detected with two commonly used algorithms were classified as monocular. Using manual inspection, the vast majority of monocular detections was easily classified as missed binocular microsaccades or noise. By visual inspection of over 800 seconds of raw pupil-, and CR data from four participants, we were not able to find a single convincing case of monocular microsaccades. Consequently, monocular detections should not readily be interpreted as monocular microsaccades, which may be a red herring in microsaccade research.

4.2. Acknowledgments

We are indebted to SR Research for excellent support when helping us to access and interpret raw data acquired from the eye tracker. The authors gratefully acknowledge the Lund University Humanities Lab, Lund, Sweden, where the data were recorded. Author RA acknowledges support from the Swedish Research Council, Grant Number 437-2014-6735.

5. References

Abadi, R., & Gowen, E. (2004). Characteristics of saccadic intrusions. *Vision research*, *44*, 2675–2690.

Bahill, A. T., Clark, M. R., & Stark, L. (1975). The main sequence, a tool for studying human eye movements. *Mathematical Biosciences*, *24*, 191–204.

Bahill, A. T., Kallman, J. S., & Lieberman, J. E. (1982). Frequency limitations of the two-point central difference differentiation algorithm. *Biological cybernetics*, *45*, 1–4.

Collewijn, H., Erkelens, C. J., & Steinman, R. (1988). Binocular co-ordination of human horizontal saccadic eye movements. *The Journal of Physiology*, *404*, 157–182.

Collewijn, H., & Kowler, E. (2008). The significance of microsaccades for vision and oculomotor control. *Journal of Vision*, *8*, 20.

Cullen, K. E., & Van Horn, M. R. (2011). The neural control of fast vs. slow vergence eye movements. *European Journal of Neuroscience*, *33*, 2147–2154.

Ditchburn, R., & Foley-Fisher, J. (1967). Assembled data in eye movements. *Journal of Modern Optics*, *14*, 113–118.

Engbert, R., & Kliegl, R. (2003a). Binocular coordination in microsaccades. *The mind's eyes: Cognitive and applied aspects of eye movements*, (pp. 103–117).

Engbert, R., & Kliegl, R. (2003b). Microsaccades uncover the orientation of covert attention. *Vision Research*, *43*, 1035–1045.

Engbert, R., & Mergenthaler, K. (2006). Microsaccades are triggered by low retinal image slip. *Proceedings of the National Academy of Sciences*, *103*, 7192–7197.

Gautier, J., Bedell, H. E., Siderov, J., & Waugh, S. J. (2016). Monocular microsaccades are visual-task related. *Journal of vision*, *16*, 37–37.

Hooge, I., Holmqvist, K., & Nyström, M. (2016). The pupil is faster than the corneal reflection (cr): Are video based pupil-cr eye trackers suitable for studying detailed dynamics of eye movements? *Vision research*, *128*, 6–18.

Hooge, I. T. C., Niehorster, D. C., Nyström, M., Andersson, R., & Hessels, R. S. (in press). Is human classification a gold standard in fixation detection? *Behavior Research Methods*, .

King, W. (2011). Binocular coordination of eye movements–hering's law of equal innervation or uniocular control? *European Journal of Neuroscience*, *33*, 2139–2146.

Kloke, W. B., Jaschinski, W., & Jainta, S. (2009). Microsaccades under monocular viewing conditions. *Journal of Eye Movement Research*, *3*, 1–7.

Krauskopf, J., Cornsweet, T. N., & Riggs, L. A. (1960). Analysis of eye movements during monocular and binocular fixation. *Journal of the Optical Society of America*, *50*.

Martinez-Conde, S., Macknik, S., Troncoso, X. G., & Hubel, D. H. (2009). Microsaccades: a neurophysiological analysis. *Trends in neurosciences*, *32*, 463–475.

Martinez-Conde, S., Macknik, S. L., & Hubel, D. H. (2004). The role of fixational eye movements in visual perception. *Nature Reviews Neuroscience*, *5*, 229–240.

Martinez-Conde, S., Macknik, S. L., Troncoso, X. G., & Dyar, T. A. (2006). Microsaccades counteract visual fading during fixation. *Neuron*, *49*, 297–305.

Martinez-Conde, S., Otero-Millan, J., & Macknik, S. L. (2013). The impact of microsaccades on vision: towards a unified theory of saccadic function. *Nature Reviews Neuroscience*, *14*, 83–96.

McCamy, M. B., Otero-Millan, J., Leigh, R. J., King, S. A., Schneider, R. M., Macknik, S. L., & Martinez-Conde, S. (2015). Simultaneous recordings of human microsaccades and drifts with a contemporary video eye tracker and the search coil technique. *PloS one*, *10*, e0128428.

Merchant, J., Morrissette, R., & Porterfield, J. L. (1974). Remote measurement of eye direction allowing subject motion over one cubic foot of space. *Biomedical Engineering, IEEE Transactions on*, (pp. 309–317).

Møller, F., Laursen, M., Tygesen, J., & Sjølie, A. (2002). Binocular quantification and characterization of microsaccades. *Graefe's archive for clinical and experimental ophthalmology*, *240*, 765–770.

Nyström, M. (2017). Monocular microsaccades. Retrieved from osf.io/ayjs9.

Nyström, M., Andersson, R., Magnusson, M., Pansell, T., & Hooge, I. (2015). The influence of crystalline lens accommodation on post-saccadic oscillations in pupil-based eye trackers. *Vision research*, *107*, 1–14.

Nyström, M., Hansen, D. W., Andersson, R., & Hooge, I. (2014). Why have microsaccades become larger? investigating eye deformations and detection algorithms. *Vision research*, .

Nyström, M., Hooge, I., & Andersson, R. (2016). Pupil size influences the eye-tracker signal during saccades. *Vision research*, *121*, 95–103.

Nyström, M., Hooge, I., & Holmqvist, K. (2013). Post-saccadic

oscillations in eye movement data recorded with pupil-based eye trackers reflect motion of the pupil inside the iris. *Vision Research*, *92*, 59–66.
Otero-Millan, J., Castro, J. L. A., Macknik, S. L., & Martinez-Conde, S. (2014). Unsupervised clustering method to detect microsaccades. *Journal of vision*, *14*, 18.
Peirce, J. W. (2007). Psychopy—psychophysics software in python. *Journal of neuroscience methods*, *162*, 8–13.
Peirce, J. W. (2008). Generating stimuli for neuroscience using psychopy. *Frontiers in neuroinformatics*, *2*, 10.
Poletti, M., & Rucci, M. (2016). A compact field guide to the study of microsaccades: Challenges and functions. *Vision research*, *118*, 83–97.
Rolfs, M. (2009). Microsaccades: small steps on a long way. *Vision research*, *49*, 2415–2441.
Rolfs, M., Kliegl, R., & Engbert, R. (2008). Toward a model of microsaccade generation: The case of microsaccadic inhibition. *Journal of Vision*, *8*, 5–5.
Rucci, M., & Victor, J. D. (2015). The unsteady eye: an information-processing stage, not a bug. *Trends in neurosciences*, *38*, 195–206.
Savitzky, A., & Golay, M. J. (1964). Smoothing and differentiation of data by simplified least squares procedures. *Analytical chemistry*, *36*, 1627–1639.
Scholes, C., McGraw, P. V., Nyström, M., & Roach, N. W. (2015). Fixational eye movements predict visual sensitivity. In *Proc. R. Soc. B* (p. 20151568). The Royal Society volume 282.
Siegenthaler, E., Costela, F. M., McCamy, M. B., Di Stasi, L. L., Otero-Millan, J., Sonderegger, A., Groner, R., Macknik, S., & Martinez-Conde, S. (2014). Task difficulty in mental arithmetic affects microsaccadic rates and magnitudes. *European Journal of Neuroscience*, *39*, 287–294.
Skavenski, A., Hansen, R., Steinman, R. M., & Winterson, B. J. (1979). Quality of retinal image stabilization during small natural and artificial body rotations in man. *Vision research*, *19*, 675–683.
Troncoso, X. G., Macknik, S. L., & Martinez-Conde, S. (2008). Microsaccades counteract perceptual filling-in. *Journal of Vision*, *8*, 15–15.
Van Horn, M. R., & Cullen, K. E. (2012). Coding of microsaccades in three-dimensional space by premotor saccadic neurons. *Journal of Neuroscience*, *32*, 1974–1980.
Young, L. R., & Sheena, D. (1975). Survey of eye movement recording methods. *Behavior Research Methods & Instrumentation*, *7*, 397–429.

AppendixA.

Figure A.10 illustrates how the length of the Savitzky-Golay filter influences the rate of detected microsaccades using the EK-algorithm. The maximum rates are reached for filter lengths between 20–25 ms.

We also tried to input 'raw', unfiltered gaze data to the microsaccade detection algorithm by Otero-Millan et al. (2014). Raw data can be recorded by turning off both heuristic filter in the EyeLink software. As is shown in Table A.6, using raw data increases the number of monocular detections considerably, while at the same time decreases the number of binocular detections (compare with Table 3).

Figure A.11 shows four cases of raw data where it could not excluded that a monocular microsaccade was performed. The detections were performed by human coders.

Table A.6: Microsaccade statistics using raw, unfiltered data as input. Microsaccades were detected with the algorithm by Otero-Millan et al. (2014). Amplitudes are in minutes.

PID	Eye	N	Rate	Amp (M ± SD)
P_1	L	265	0.65	6.30 ± 4.25
	R	215	0.53	7.75 ± 4.81
	B	228	0.56	9.82 ± 3.99
P_2	L	48	0.12	21.19 ± 10.54
	R	163	0.40	20.87 ± 20.99
	B	395	0.97	43.47 ± 24.50
P_3	L	13	0.03	17.00 ± 8.23
	R	440	1.10	6.97 ± 5.17
	B	126	0.32	20.07 ± 10.06
P_4	L	822	2.02	6.37 ± 4.37
	R	145	0.36	9.84 ± 5.84
	B	182	0.45	11.69 ± 8.02
P_5	L	5	0.03	10.44 ± 4.67
	R	103	0.53	7.52 ± 5.66
	B	70	0.36	33.14 ± 30.62
P_6	L	65	0.33	10.99 ± 5.45
	R	72	0.36	11.24 ± 4.68
	B	126	0.63	15.42 ± 5.56
P_7	L	299	1.58	7.79 ± 5.08
	R	278	1.47	7.53 ± 4.83
	B	286	1.51	10.09 ± 5.52
P_8	L	58	0.15	12.84 ± 6.77
	R	92	0.24	14.94 ± 8.04
	B	192	0.50	23.26 ± 12.98

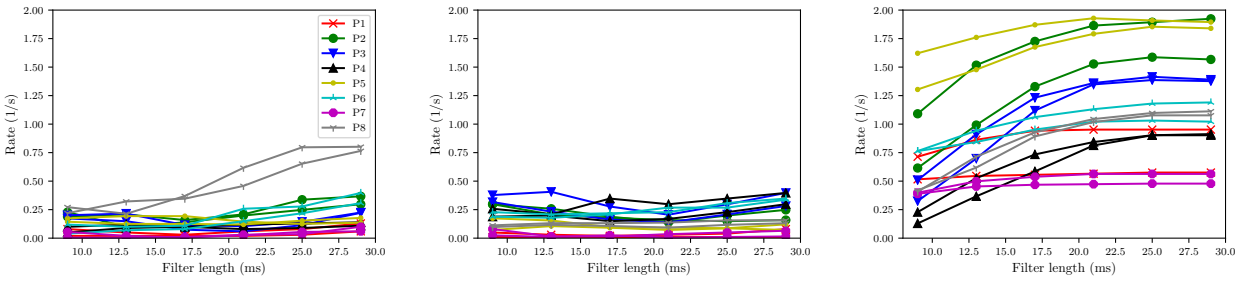

(a) Left eye (b) Right eye (c) Binocular

Figure A.10: Influence of the length of the Savitzky-Golay filter on the rate of monocular (a, b) and binocular (c) detections. There are two lines for each participant; one for each block.

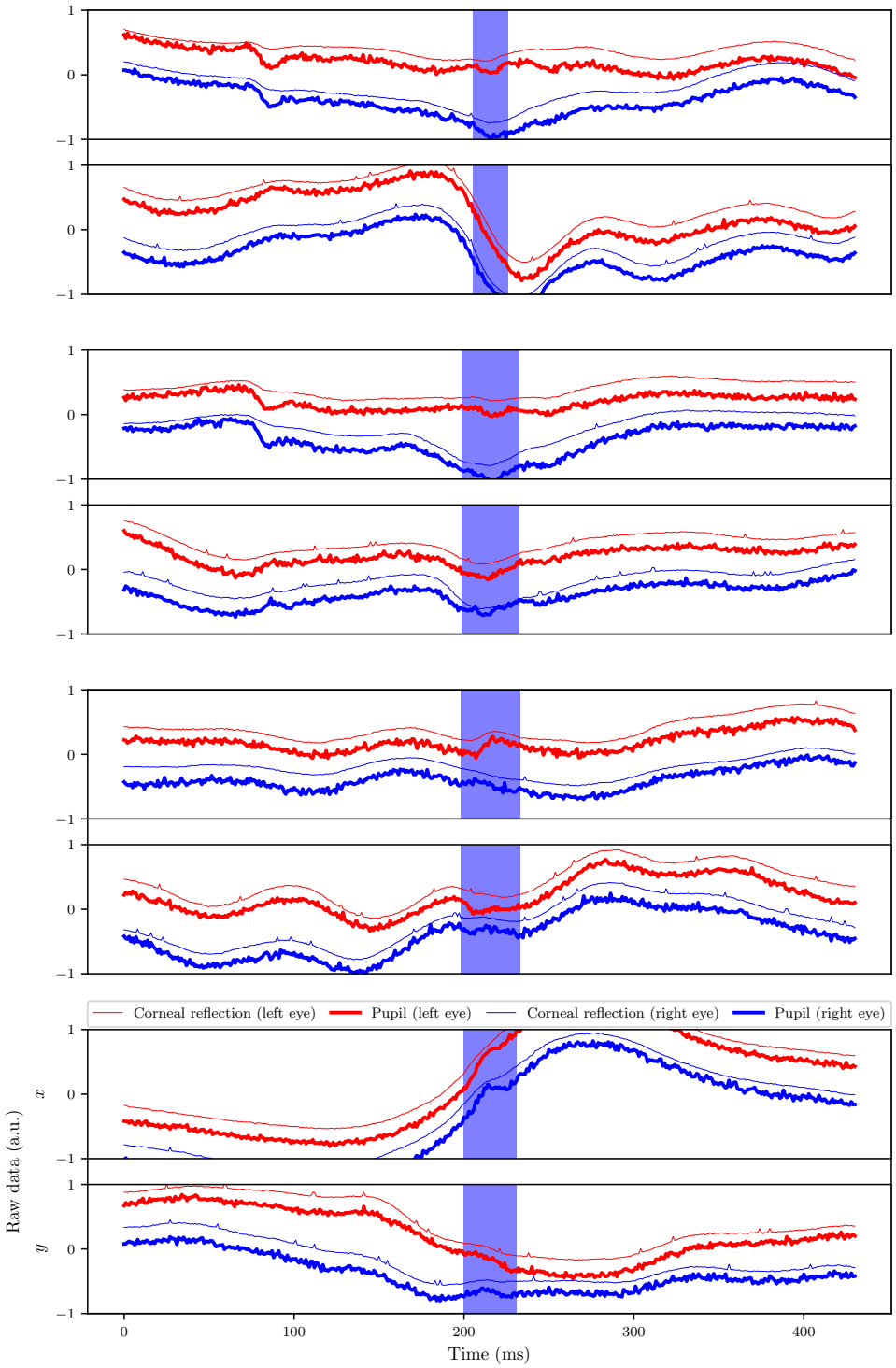

Figure A.11: The four instances in the raw pupil- and CR-signals marked as possible monocular microsaccades during manual coding. The blue vertical bars span the detected events.